12

Spectro-Electrochemical Investigation of the bc_1 Complex from the yeast *Saccharomyces cerevisiae* using Surface Enhanced B-Band Resonance Raman Spectroscopy

Denise Schach[1,2], Marc Großerüschkamp[1,2], Christoph Nowak[1,2], Wolfgang Knoll[2] and Renate L. C. Naumann[1,2]
[1]*Max Planck Institute for Polymer Research, Ackermannweg 10, 55128 Mainz,*
[2]*Austrian Institute of Technology GmbH – AIT, Donau-City Str. 1, 1220 Vienna,*
[1]*Germany*
[2]*Austria*

1. Introduction

The ubiquinol-cytochrome c oxidoreductase (bc_1 complex), also denoted complex III of the respiratory chain, is present in the inner mitochondrial membrane of eukaryotic organisms and many aerobic bacteria. It catalyzes electron transfer from ubiquinol to cytochrome c coupled to the electrogenic translocation of protons across the membrane. The proton electrochemical gradient thus generated is used for the synthesis of ATP. The crystal structure of the bacterial and the mitochondrial bc_1 complex was determined by X-ray diffraction.(Xia, Yu et al. 1997; Hunte, Koepke et al. 2000; Lange and Hunte 2002; Palsdottir, Lojero et al. 2003; Berry, Huang et al. 2004; Solmaz and Hunte 2008) Both are present as a dimer, the mitochondrial complex differs from the bacterial one by a larger number of subunits extending into the aqueous phase. The elements essential for the function of the enzyme such as the location and orientation of the redox centers, however, are very similar. Three of the four prosthetic groups of the bc_1 complex, heme b_l and b_h and cytochrome c_1, are metalloporphyrins.. Vibrational modes of metalloporphyrins have been extensively studied by Resonance Raman (RR) spectroscopy, since specific modes are very sensitive to the redox state of the heme structure.(Kitagawa, Kyogoku et al. 1975; Spiro 1975; Kitagawa, Ozaki et al. 1978; Spiro 1978) RR spectra were obtained mostly from B-band (Soret) excitations,(Spiro 1988) whereas Q-band excited spectra are less intensive and informative at low protein concentrations.(Le Moigne, Schoepp et al. 1999) Soret excitation and Q-band resonance was applied for investigations of the bacterial (Hobbs, Kriauciunas et al. 1990; Le Moigne, Schoepp et al. 1999) and mitochondrial bc_1 complex (Gao, Qin et al. 1998), respectively. In these cases the redox state of the hemes was altered by adding soluble redox compounds such as ascorbate and sodium hydrosulphite to the protein, which was present in the detergent-solubilized form. By contrast in the present investigation we use electrochemistry to direct electron transfer (ET) into the enzyme reconstituted into a lipid bilayer, a method that we had introduced successfully in the case of cytochrome c

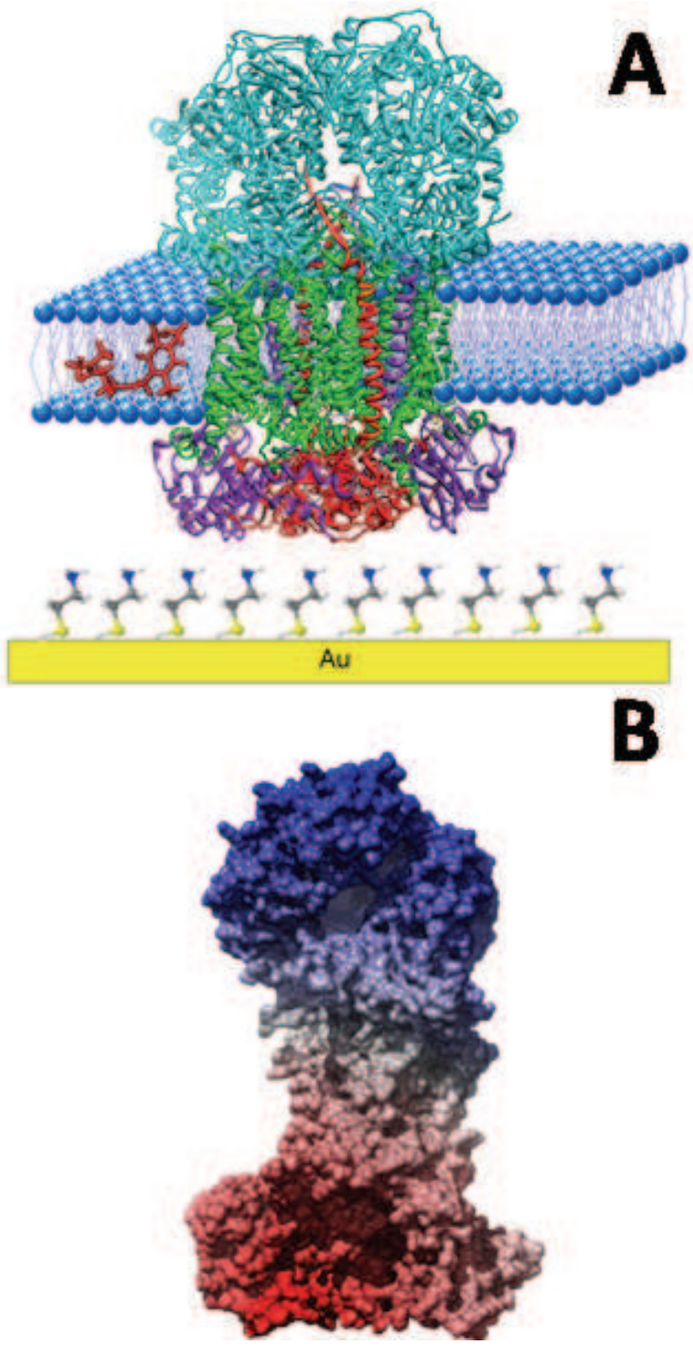

Fig. 1. **Ubiquinol-cytochrome c oxidoreductase** . (A) Cytochrome bc_1 complex from the yeast *Saccharomyces cerevisiae* (Lange and Hunte 2002) adsorbed onto a cysteamine functionalized electrode and reconstituted into a bilayer lipid membrane.The protein is assembled with the intermembrane side directed toward the electrode. Ubiquinone Q_{10} (dark red) is incorporated into the bilayer lipid membrane. (B) Electrostatic surface of the monomer of the yeast bc_1 complex(Lange, Nett et al. 2001) in the equivalent orientation. The intermembrane side comprises a negatively charged surface (red) whereas the matrix site comprises a positively charged surface (blue).

oxidase.(Friedrich, Robertson et al. 2008; Nowak, Schach et al. 2009; Schach, Nowak et al. 2010) For this purpose the bc_1 complex from the yeast *Saccharomyces cerevisiae* was adsorbed on a monolayer of cysteamine (CA) self assembled on template stripped gold (TSG) and alternatively the top plane of a silver rod modified with silver nanoparticles (Fig. 1A). This way the bc_1 complex is immobilized in a preferred orientation due to electrostatic interaction between the negatively charged surface of the protein and the positively charged CA layer (Fig. 1B shows the electrostatic surface charge distribution). The silver rod works at the same time as an electrode and due to the modification with the nanoparticles as the active surface for purposes of Surface Enhanced Resonance Raman Spectroscopy (SERRS).(Grosserueschkamp, Nowak et al. 2009) After immobilization the protein is reconstituted into a protein-tethered bilayer lipid membrane (ptBLM) using in-situ dialysis of micelles prepared from a lipid with the help of a detergent. The formation of the ptBLM is controlled by surface plasmon resonance (SPR) and electrochemical impedance spectroscopy (EIS) (Fig. 2A, B, C, respectively). Cyclic voltammetry (CV) measurements (Fig. 3) as well as potentiometric titrations are performed, i.e. SERR spectra of the biomimetic membrane system are measured at different potentials applied to the electrode (Fig. 4-6). Spectra are analyzed on the basis of previous investigations of the bc_1 complex in different oxidation states obtained by adding reducing compounds in solution.(Hobbs, Kriauciunas et al. 1990; Le Moigne, Schoepp et al. 1999) These data are used to find out whether or not electrochemical reduction/oxidation of the bc_1 complex can be accomplished under the experimental conditions described above.

2. Materials and methods

Electrochemical measurements (EIS and CV) were performed on template stripped gold (TSG) electrodes, whereas potentiometric titrations followed by SERRS were conducted on the top plane surfaces of silver rods modified with AgNPs.

Modification of the silver electrodes was done as described.(Grosserueschkamp, Nowak et al. 2009) The top planes of 12 mm thick silver rods were polished down to an rms roughness of 3-5 nm.(Grosserueschkamp, Friedrich et al. 2009) Self-assembled monolayers (SAMs) of cysteamine (CA) were formed on the silver rods by immersion into an aqueous solution of CA (10 mM/l) for 1 h. After thorough rinsing with water the modified silver surfaces were immersed for two hours into a suspension of silver nanoparticles of 40 nm diameter. Thereafter the silver rods were again rinsed with water.

Immobilization of the protein and reconstitution into a lipid bilayer: Either TSG electrodes or the above mentioned silver electrodes modified with nanoparticles were immersed for 1 h into a solution of CA 10 mM/L. The excess CA was removed by rinsing the surfaces with water. The bc_1 complex from the yeast *Saccharomyces cerevisiae* was expressed and purified according to the method of H. Pálsdóttir and C. Hunte.(Pálsdóttir and Hunte 2003) The protein was adsorbed by exposing either the gold electrode or the silver surfaces for 1h to a solution of bc_1 complex (0.1 µM/l) in phosphate / dodecyl-D-maltoside (DDM) buffer (K_2HPO_4 0.05 M/l, KCl 0.1 M/l, pH = 7, 0.1% DDM). The protein solution was removed by cautious rinsing with PBS / DDM buffer. The detergent solution was then replaced by a lipid-containing PBS / DDM buffer (K_2HPO_4 (Sigma Aldrich) 0.05 M/l, KCl (Sigma Aldrich) 0.1 M/l, pH = 7, 0.1% DDM (Sigma Aldrich), DiPhyPC (Avanti Polar Lipids) 0.05 mg/ml). Ubiquinone Q_{10} (Fluka) was added if mentioned in the text to the lipid-containing PBS at a concentration of 0.025 mg/ml. Biobeads (Bio-Rad Laboratories GmbH,

Munich, Germany) were added to initiate dialysis. Membrane formation was finished after 24 hours. Thereafter the excess lipid buffer and the biobeads were removed by rinsing with fresh PBS buffer.

Surface Plasmon Resonance (SPR): SPR was performed in a custom-made setup using the Kretschmann-configuration. The glass slide (LaSFN9 glass from Hellma Optik, Jena, refractive index n = 1.85 at 633 nm) was optically matched to the base of a 90° glass prism (LaSFN9). Monochromatic light from a He/Ne Laser, (Uniphase, San Jose, CA, λ = 632.8 nm) was directed through the prism and collected by a custom made photodiode detector. Reflectivity at a fixed angle of incidence transferred into a thickness yields the time course of protein binding and reconstitution.

Electrochemistry: Electrochemical measurements were performed using an Autolab instrument (PGSTAT302) equipped with an FRA2-Module for electrochemical impedance measurements, an ECD-module amplifier for low-currents, an ADC750 module for rapid scan measurements and a SCAN-GEN module for analog potential scanning. Electrochemical impedance spectroscopy (EIS) data were recorded in a frequency range of 50 kHz – 3 mHz with an excitation amplitude of 10 mV and a bias potential of 0 V against an $Ag|AgCl,KCl_{sat}$ reference electrode. Data were analyzed by the complex nonlinear fitting algorithm supplied in the data processing software ZVIEW (Version 2.6, Scribner Associates, Inc.). Cyclic voltammetry experiments were conducted with IR drop compensation. Measurements under anaerobic conditions were performed in a buffer solution containing K_2HPO_4 0.05 Mol/l, KCl 0.1 Mol/l, pH = 7 and the oxygen trap consisting of glucose (0.3% w/w) (Sigma Aldrich), glucose oxidase (75 µg/ml) (Sigma Aldrich) and catalase (12.5 µg/ml) (Sigma Aldrich). This solution was flushed with Ar purged from oxygen by bubbling through the oxygen trap containing buffer solution. All electrochemical measurements were taken in a three electrode configuration with gold as the working electrode, an $Ag|AgCl,KCl_{sat}$ reference and a platinum wire as the counter electrode. All electrode potentials are quoted versus SHE.

Spectro-electrochemical Raman measurements: The measurements were performed under anaerobic conditions as described above for electrochemical measurements. The spectra were recorded at room temperature. The setup, used for the Raman measurements was described in detail in a previous publication.(Grosserueschkamp, Friedrich et al. 2009) The 413 nm emission line of a Kr^+ laser (Innova 90C, Coherent) was used for the Soret excitation. After passing a premonochromator (Laserspec III, Spectrolab Research Laboratory, Newbury, England) the laser beam was coupled into a confocal Raman microscope (LabRam, HR800, HORIBA Jobin Yvon) equipped with a water immersion objective (Olympus LUMPLFL, 100 XW, WD = 1.5, NA = 1, BFOBJ). By this means the laser beam with a power of 3 mW was focused on top of the prepared plane of the silver rod. The scattered light was filtered by a holographic notch filter and guided to an 1800 grooves/mm grating providing spectral resolution. The spectra were imaged onto a liquid nitrogen cooled back-illuminated CCD detector (Symphony, Jobin Yvon). Spectro-electrochemical measurements were taken in a three electrode configuration with silver as the working electrode, an $Ag|AgCl,KCl_{sat}$ reference and a platinum wire as the counter electrode. Potentials were applied by using a software controlled (GPES, Autolab) potentiostat (Autolab, PGSTAT302, Eco Chemie, B.V., Utrecht, Netherlands). All electrode potentials are quoted versus SHE.

3. Results

3.1 SPR/EIS measurements

Adsorption of the bc_1 complex solubilized in DDM on the monolayer of CA was recorded by SPR (Fig. 2A). The kinetic trace shows a thickness increase due to bc_1 complex adsorption, however, saturation was not attained indicating unspecific adsorption. In order to avoid too much unspecific binding, the adsorption process was cut short at about the beginning of the saturation and the excess protein was washed off with DDM containing PBS buffer. In-situ dialysis initiated by adding biobeads was indicated by a further increase of the reflectivity definitely reaching saturation after a period of 20 hrs. This is characteristic for the exchange of detergent by lipid molecules in the protein monolayer as we had observed in the case of proteins specifically adsorbed using the his-tag technology. The thickness of the protein layer obtained from fitting the angle scans of 10 nm (inset of Fig. 2A) indicates a submonolayer of bc_1 complex considering a thickness of the protein of 18 nm according to X-ray data (Chase and Parkinson 1991; Feng and Tachikawa 2008) (Table 1). A further thickness increase by 2 nm after dialysis characterizes the formation of lipid bilayer patches between immobilized proteins. These findings are confirmed by electrochemical impedance spectroscopy showing a decrease of the capacitance and an increase of the resistance after dialysis (Fig. 2B, C). The sealing resistance in the order of magnitude of several $M\Omega cm^2$ is well in the range of resistances, that we had found in the case of ptBLMs based on his-tagged proteins (Table 1). The decrease of the capacitance and the increase of the resistance can be explained in terms of the difference in the dielectric constants of the protein ($\varepsilon = 20$) and lipid ($\varepsilon = 2$). The capacitance decreases since detergent and water are replaced by lipid molecules. We conclude that a densely packed mixed protein/lipid bilayer had been formed on the surface.

3.2 Cyclic voltammetry

Cyclic voltammograms were performed at pH = 7 under anaerobic conditions. They showed a slow process at around -400 mV vs. SHE (Fig. 3), which was attributed to the uptake of two electrons and two protons by ubiquinone Q_{10} to form ubihydroquinone. Midpoint potentials from +265 mV to +300 mV and from +190 mV to +290 mV were reported for heme c_1 and the Rieske center, respectively, whereas -30 mV to +100 mV, and -90 mV to -30 mV were found for heme b_H and b_L, respectively.(Hobbs, Kriauciunas et al. 1990; Le Moigne, Schoepp et al. 1999) So obviously, the b-type hemes do not exchange electrons directly with the electrode. In order to find out about ubiquinone Q_{10}, we added this coenzyme to the lipid/DDM buffer solution used for dialysis. Ubiquinone is thus incorporated into the mixed protein-lipid layer, as shown by two well defined cathodic peaks at about -0.35 V and -0.55 V in the CV. These peaks were attributed to the stepwise electrochemical reduction of ubiquinone Q_{10} to ubisemiquinone and ubihydroquinone, respectively. The cathodic peaks decrease with successive scans, which is considered as an indication of the reduced species of ubiquinone Q_{10} being consumed by the enzyme (see Fig. 3, inset). The cathodic peaks are accompanied by a couple of small peaks at +250 mV and +350 mV, which are tentatively attributed to the heme c_1. It should be noted that ubiquinone Q_{10} neither in the oxidized nor reduced form added to the aqueous buffer solution gives rise to any response in the CVs. Hence the presence of these peaks in the CV alone are a clear indication of a lipid layer around the proteins. Ubiquinone Q_{10} dissolved in the lipid phase can thus exchange electrons with the electrode to form ubisemiquinone and ubihydroquinone. The formation of the reduced forms of ubiquinone Q_{10} opens the possibility of the hemes being reduced electrochemically mediated by ubihydroquinone.

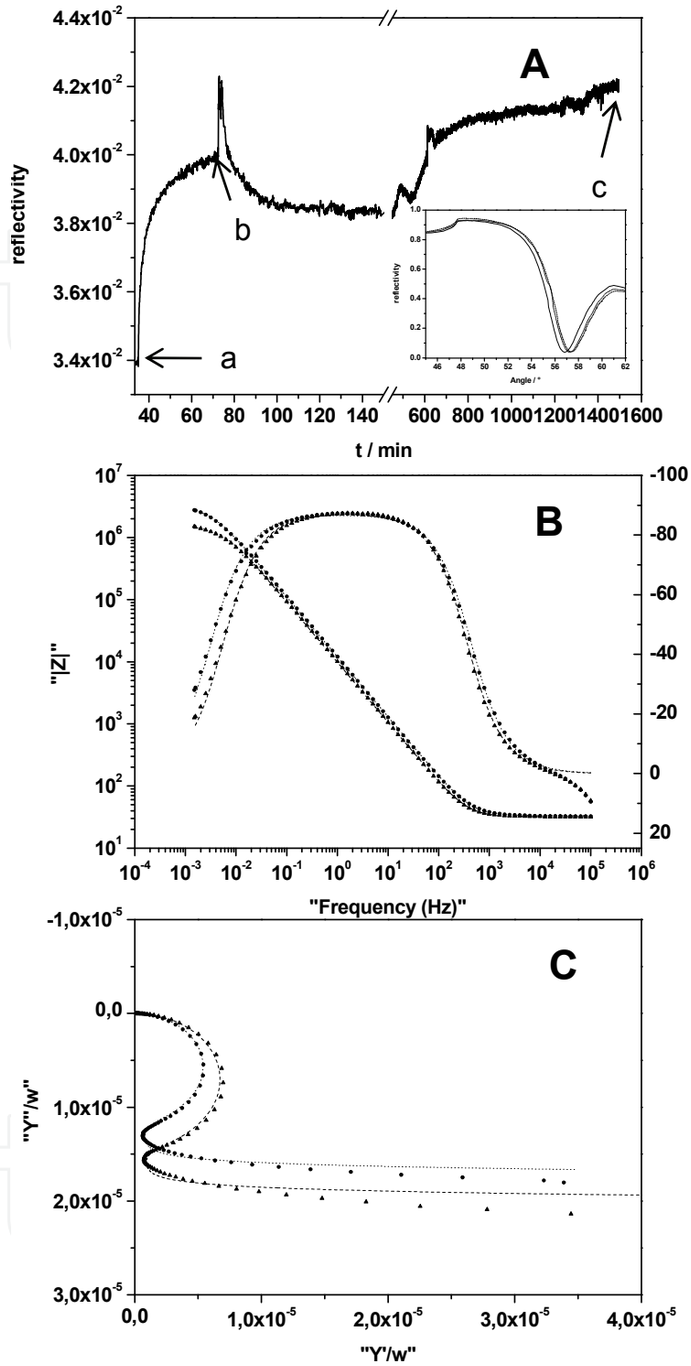

Fig. 2. **Immobilization of bc_1 complex and reconstitution into the ptBLM.** (A) Kinetic trace of the SPR spectrum at a fixed angle of incidence Θ = 54° showing the adsorption of the bc_1 complex in solubilized form before (a) and after (b) addition of the protein and the reconstitution of a lipid bilayer (c) after the addition of biobeads to the lipid-detergent containing buffer solution. (B) Bode plot and (C) frequency normalized admittance plot of electrochemical impedance spectra after adsorption of bc_1 complex (solid triangles) and after reconstitution (solid circles).

	C/μF cm^{-2}	R/MΩ cm^2	Δd / nm (theory)	Δd / nm (exp.)
spacer molecule			0.6	0.5
bc_1 complex	17.1+/- 0.1	1.5+/- 0.2	18.0 (Hunte, Koepke et al. 2000)	10.0
lipid bilayer	14.2 +/- 0.1	3.1+/- 0.4	2.0	2.0

Table 1. Data from EIS and SPR measurements of the different layer structures

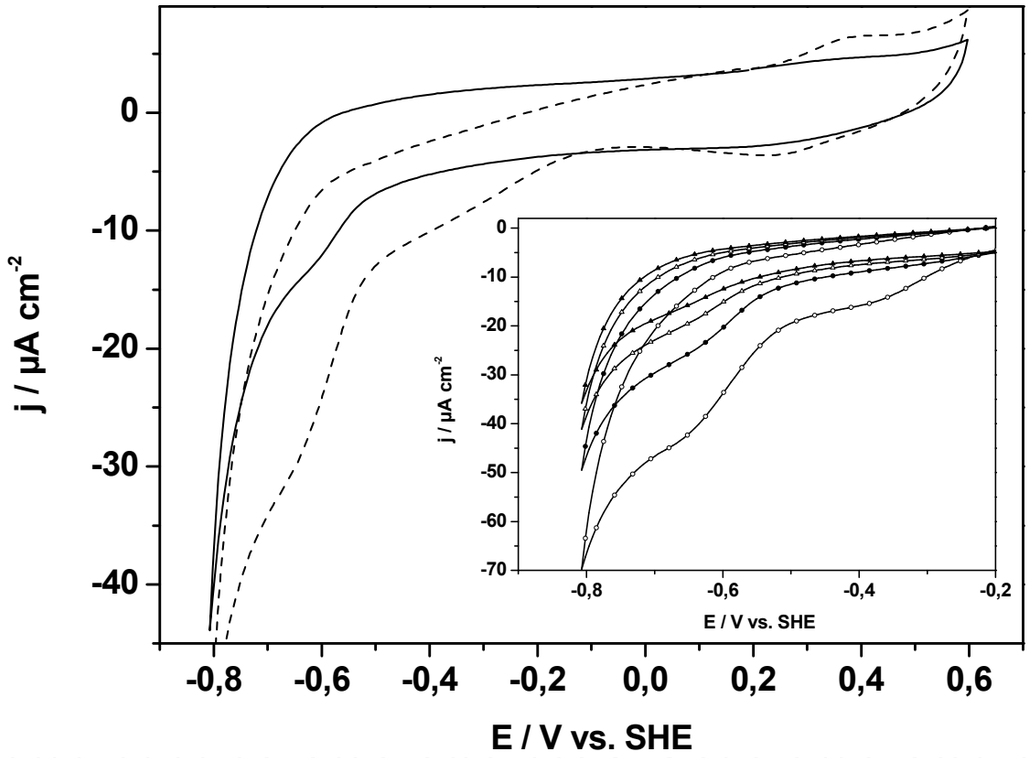

Fig. 3. **Cyclic voltammograms of bc_1 complex** adsorbed onto a functionalized electrode and reconstituted into a bilayer lipid membrane (see Fig.1) with additional ubiquinone Q_{10} (dashed line and inset) and without additional ubiquinone Q_{10} (solid line) taken under anaerobic conditions (2nd scans at scan rate 0.05 Vs^{-1} for either CV). The inset shows evolution of the CVs after insertion of ubiquinone Q_{10} to the protein-lipid layer. 1st scan (open circles), 2nd scan (solid circles), 3rd scan (open triangles) and 4th scan (solid triangles).

3.3 Resonance Raman study

SERR spectra were recorded at 250 mV for the oxidized heme species and at -400 mV for the reduced heme species (Fig. 4A-D). At these potentials the enzyme was found to be in the fully oxidized and reduced form, respectively, see below for the details. The spectra were

sub-divided into different ranges for better interpretation. Tentative band assignments were performed according to SERR spectra obtained from two different sources both using the bacterial bc_1 complex (Hobbs, Kriauciunas et al. 1990; Le Moigne, Schoepp et al. 1999) from *Rhodospirillum rubrum* under conditions mentioned above (Table 2).

In general, frequency modes observed upon B-band excitations over the entire frequency range showed band profiles with higher intensities at the negative potential than at the positive potential (Fig. 4). This phenomenon is associated with the potential dependent surface enhancement effect, which is well known to result from two main effects: an electromagnetic effect and a chemical effect.(Chase and Parkinson 1991; Feng and Tachikawa 2008) On the basis of intensity versus potential profiles measured in electrochemical environments, it has been shown, that the charge transfer mechanism dominates the intensity of SERR spectra of molecules adsorbed on a silver electrode. (Lombardi, Birke et al. 1986; Osawa, Matsuda et al. 1994)

Low Frequency Region (250 – 450 cm^{-1})

SERR spectra of the bc_1 complex measured in this region are shown in (Fig. 4A). Distortion of the heme groups effect the majority of bands occurring at these frequencies.(Hu, Morris et al. 1993) In general the region below 1000 cm^{-1} comprises modes with less enhancement since these are stronger coupled to ring deformations and stretching of bonds to the central metal iron than to $\pi-\pi^*$ excitations, as it is the case in the high frequency region. Furthermore a natural falloff of Raman intensity with decreasing frequency is noted in literature.(Choi and Spiro 1983)

The ν_9 mode, a $\delta(C_\alpha-C_m)_{sym}$ vibration, (Spiro, Czernuszewicz et al. 1989) is displayed in the measured spectra at 263 cm^{-1} for the oxidized state and at 265 cm^{-1} for the reduced state. The ν_9 mode is a peripheral heme mode that occurs distinctly for b-type hemes.

For the reduced heme species five prominent overlapping bands arise between 343 cm^{-1} and 416 cm^{-1}, whereas two bands of this profile, at 343 cm^{-1} and 407 cm^{-1} only persist in the spectra recorded for the oxidized state. The band at 343 cm^{-1} appears for either of the redox states. In both cases it can be assigned to the ν_8 mode of b- and c-type cyt. The ν_8 mode, a skeletal in-plane heme mode, is known to be the strongest low-frequency band in metalloporphyrin spectra. (Hu, Smith et al. 1996) This was confirmed by the present investigation.

Either the ν_8 or the ν_9 mode consist of a combination of iron-N (pyrrole) stretching and C_b-pyrrole-substituent deformation.(Hu, Morris et al. 1993) Previous measurements taken at different excitation wavelengths show three neighboring bands between 344 cm^{-1} and 356 cm^{-1}, that are assigned respectively to the ν_8 modes of the heme b_H, heme c_1 and heme b_l.(Le Moigne, Schoepp et al. 1999) The spectrum presented here comprises only two bands at 344 cm^{-1} and 356 cm^{-1}. So a distinction between the hemes was not possible.

Additionally we propose to assign the shoulder of the band referring to the ν_8 mode at 356 cm^{-1} to the ν_{50} mode, a heme skeletal mode of the reduced cyt c_1. It seems to be not existent in the spectra for the oxidized state. The region between 377 cm^{-1} and 416 cm^{-1} is dominated by deformation modes of peripheral heme groups. For the reduced species we find three bands at 377 cm^{-1}, 403 cm^{-1} and 416 cm^{-1}, that have been assigned to δ_{CPr} of heme b, $\delta_{CCaCb2,4}$ of heme c_1 and δ_{CCVn} of heme b, respectively. In the oxidized state there is one band at 407 cm^{-1} left, which we assigned to δ_{CCVn} of heme b.(Le Moigne, Schoepp et al. 1999)

In general peripheral heme modes show sensitivity to vibrations of peripheral groups, therefore they can be considered as fingerprint vibrations identifying the heme types. The assignment of bands particularly in the low frequency region demonstrates that we can distinguish between signals originating from b- or c-type hemes. We can also conclude that reduction and oxidation of both types of hemes are reduced and oxidized in this particular potential window.

Mid Frequency Region (450 – 1250 cm^{-1})

The mid frequency region (Fig. 4B and C) can be sub-divided into two parts. The part between 450 cm^{-1} and 920 cm^{-1} is dominated by heme skeletal modes, whereas the spectrum between 920 cm^{-1} and 1250 cm^{-1} comprises mostly peripheral heme modes. The region between 600 cm^{-1} and 850 cm^{-1} is remarkably rich due to narrow overlapping bands with strong intensities and good signal-to-noise ratio.

A notably large band particularly for the reduced state was displayed at 681 cm^{-1}. This band was assigned to the ν_7 mode exclusively of b-type hemes.(Le Moigne, Schoepp et al. 1999) It is clearly distinguished from the ν_7 mode of heme c_1, which appears with less intensity at 697 cm^{-1} and is only existent for the reduced species.(Le Moigne, Schoepp et al. 1999) This was confirmed by a comparative measurement of the bc1 complex with cytochrome c both in the reduced state (Fig. 5, spectrum a, b, respectively). The ν_7 mode of the c- type heme in cyt c produces a band at a higher frequency, 693 cm^{-1}, however, with less intensity. The ν_7 mode, an in-plane skeletal mode, originates from a symmetrical pyrrole deformation.

The further deconvolution of the ν_7 envelope in the reduced state reveals strongly overlapping bands originating from heme skeletal modes. Two signals at 650 cm^{-1} and 663 cm^{-1} can be allocated to γ_{20}. A second shoulder of the ν_7 envelope appears at 635 cm^{-1}, which can be assigned to ν_{48}. Other shoulders are found at higher frequencies, such as 716 cm^{-1}, 747 cm^{-1} and 783 cm^{-1} are induced respectively by γ_5, ν_{15} and ν_6. The modes ν_{15} and ν_6 are both pyrrole breathing modes.(Spiro, Czernuszewicz et al. 1989) A slight signal in the lower frequency region at 460 cm^{-1} was assigned to γ_{22}.

The region between 850 cm^{-1} and 1250 cm^{-1} contains few bands of higher intensity. We find low signals at 920 cm^{-1}, 1147 cm^{-1} and 1170 cm^{-1}. The first two frequencies can be assigned to the heme skeletal modes of reduced cytochrome c_1, ν_{46} and ν_{43}, respectively. The latter frequency was assigned in the reduced and the oxidized state to the heme skeletal mode ν_{30} of cytochromes b and c_1. The ν_{30} mode originates from an asymmetrical deformation of the pyrrole half ring, whereas the ν_{46} mode corresponds to $\delta(\text{pyrrole})_{asym}$ and the ν_{43} mode is effected by a C–Y stretching mode, $\nu(C_\beta\text{–Y})_{sym}$.(Spiro, Czernuszewicz et al. 1989) Peripheral modes of b- and c-type hemes, δ_{CPr}, ν_5 and ν_{14} give rise to bands at 968 cm^{-1} (red.state)/ 972 cm^{-1} (ox. state), 1113 cm^{-1} (red. state) and 1130 cm^{-1} (red. and ox. state), respectively. Two peripheral modes of b-type hemes produce bands at 1006 cm^{-1} (ox. state) according to δ_{CVn} and at 1222 cm^{-1}(reduced and oxidized state) according to ν_{13}. We assign a slight signal occuring at 1087 cm^{-1} in the reduced state to another peripheral heme mode, δ_{CCH3} of the c-type heme.(Le Moigne, Schoepp et al. 1999)

More bands were observed in the present investigation, that were not observed in previous studies of the bc_1 complex, e.g. in the paper of Moigne et al.(Le Moigne, Schoepp et al. 1999) These are the bands at 503 cm^{-1}, 560 cm^{-1}, 715 cm^{-1}, 741 cm^{-1}, 785 cm^{-1} and 885 cm^{-1} , which appear in the spectrum of the oxidized species and the bands at 518 cm^{-1}, 546 cm^{-1}, 562 cm^{-1}, 602 cm^{-1}, 734 cm^{-1}, 1020 cm^{-1} and 1052 cm^{-1} in the spectrum of the reduced state.

We conclude from the results presented in this section that we have isolated a band at 681 cm^{-1}, which selectively demonstrates the reduction of the b-type hemes.

High Frequency Region (1250 – 1700 cm^{-1})

SERR spectra of the bc_1 complex measured in this region are shown in (Fig. 4D). In agreement with spectra of other metalloporphyrins and heme proteins they comprise particularly modes, which are strongly enhanced and resonant with dominant Q- and B electronic transitions. Mainly in-plane ring modes coupled to $\pi-\pi^*$ excitations generate these bands.(Choi and Spiro 1983) They are produced by heme skeletal vibrations and they are barely assignable distinctly to the b- or c_1-type hemes applying Soret excitation.
Contrary to the lower frequency regions the high frequency region comprises modes, which are sensitive to oxidation or spin state, such as the heme skeletal modes $\nu_{2,}$ $\nu_{3,}$ ν_4 and ν_{10}. A small general lowering of some frequencies is caused by reduction from Fe(III) to Fe(II). This process can be explained in terms of changes in π back donation, which can be understood as an electronic transition. Larger shifts of some frequencies are induced by conversion from low- to high-spin state.(Spiro and Strekas 1974) As in previous studies the ν_4 mode serves as an oxidation state marker, whereas the ν_2 mode is rather sensitive to the spin state. Either, the ν_3 and the ν_{10} mode are sensitive to both, the oxidation and the spin state.(Spiro and Strekas 1974) The frequency according to the ν_4 mode is located at 1374 cm^{-1} in the oxidized state. Reduction gives rise to a discrete shift in frequency from 1374 cm^{-1} to 1358 cm^{-1}. From the intensity of either band one can read out the concentration of reduced or oxidized species. A residual contribution of the reduced species is still apparent in the spectrum of the fully oxidized protein due to photoreduction of a fraction of the heme sites. Laser intensity dependent photoreduction has been observed before.(Hobbs, Kriauciunas et al. 1990) The band originating from the ν_4 mode is the strongest in the high frequency region, especially in the reduced state. Calculations predict, that the ν_4 mode consists of 36% of (C_α–C_β) stretching and deformation of the pyrrole half ring, the latter plays a crucial role for the sensitivity to the oxidation state.(Kozlowski, Bingham et al. 2008) Likewise the modes ν_2, ν_3 and ν_{10} originate from C–C stretching, namely $\nu(C_\beta–C_\beta)$, $\nu(C_\alpha–C_m)_{sym}$ and $\nu(C_\alpha–C_m)_{asym}$, respectively.(Spiro, Czernuszewicz et al. 1989; Hu 1993)
4In comparison to the ν_4 mode the contribution of the ν_3 mode is rather small. For the correspondent frequency a discrete shift from 1502 cm^{-1} in the oxidized state to 1492 cm^{-1} in the reduced state can be observed.
Contrary to the modes $\nu_{3,}$ ν_4 and ν_{10}, by reducing the potential the frequency according to the ν_2 mode underlies a shift to a higher value in terms of spin state transitions, which has already been observed previously.(Grosserueschkamp, Friedrich et al. 2009) In our spectra the corresponding band observed at 1581 cm^{-1} and 1589 cm^{-1} account for oxidized and reduced species, respectively.
For the reduced species we assigned three shoulders of the band referring to ν_2 at 1559 cm^{-1}, 1606 cm^{-1} and at 1620 cm^{-1} to the ν_{38} mode, a C_β–C_β stretching, to the ν_{37} mode, an asym. C_α–C_m stretching, and to the ν_{10} mode, respectively.(Spiro, Czernuszewicz et al. 1989) In the oxidized state there is no contribution from the ν_{38} and the ν_{37} mode. The ν_{10} mode however generates a slight signal, which is discretely shifted to 1631 cm^{-1} for the oxidized species. A shoulder of the band assigned to ν_4 at 1390 cm^{-1} in the reduced state can be assigned to the ν_{29} mode, originating from a pyrrole quarter ring deformation. A small band occurring for the reduced state at 1466 cm^{-1} was assigned to the ν_{28} mode, a symmetrical C_α–C_m stretching mode.(Spiro, Czernuszewicz et al. 1989)

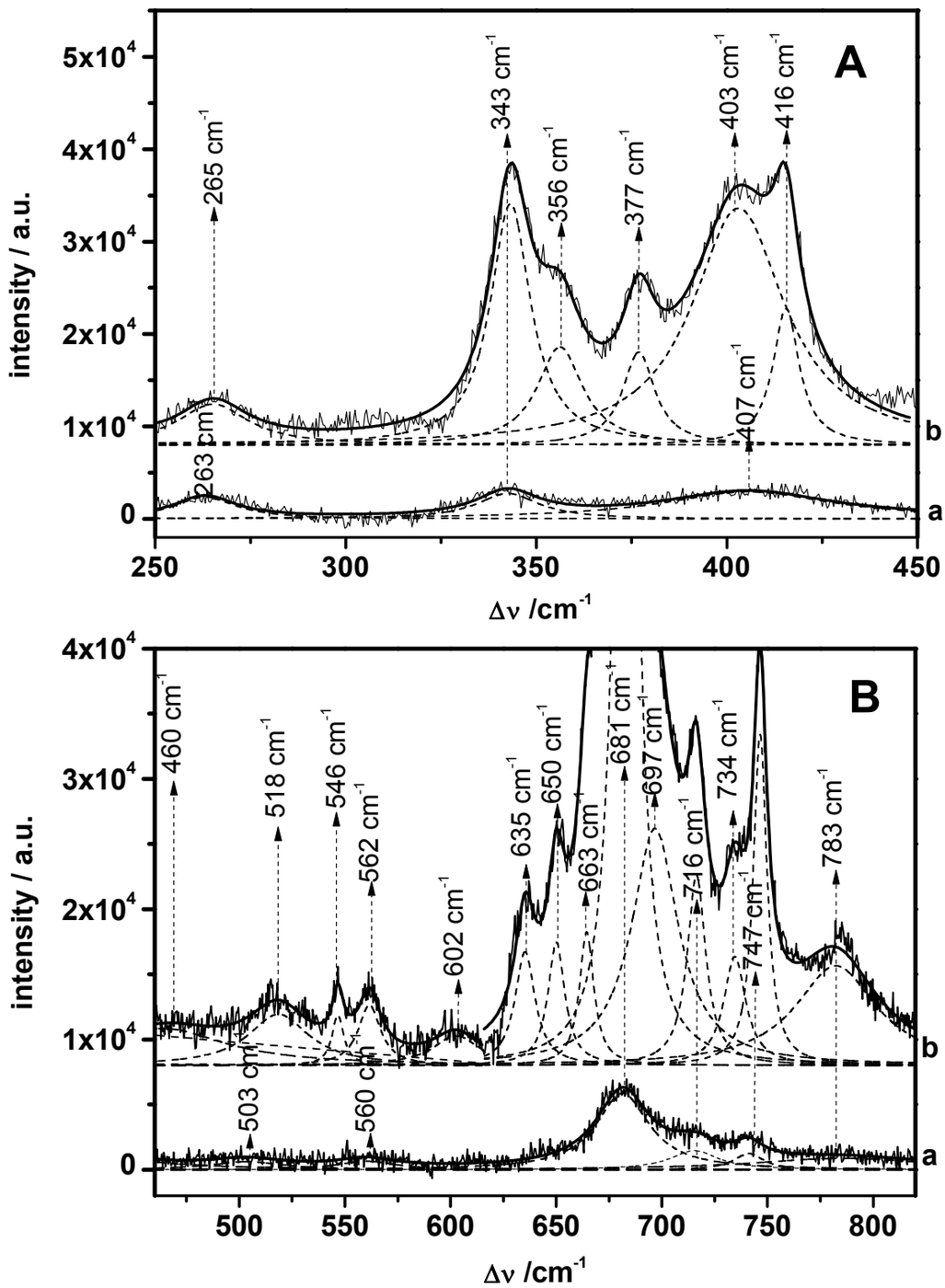
A
intensity / a.u.
Δν /cm-1
265 cm-1
343 cm-1
356 cm-1
377 cm-1
403 cm-1
416 cm-1
407 cm-1
263 cm-1
b
a
B
460 cm-1
518 cm-1
546 cm-1
562 cm-1
602 cm-1
635 cm-1
650 cm-1
663 cm-1
681 cm-1
697 cm-1
716 cm-1
734 cm-1
747 cm-1
783 cm-1
503 cm-1
560 cm-1

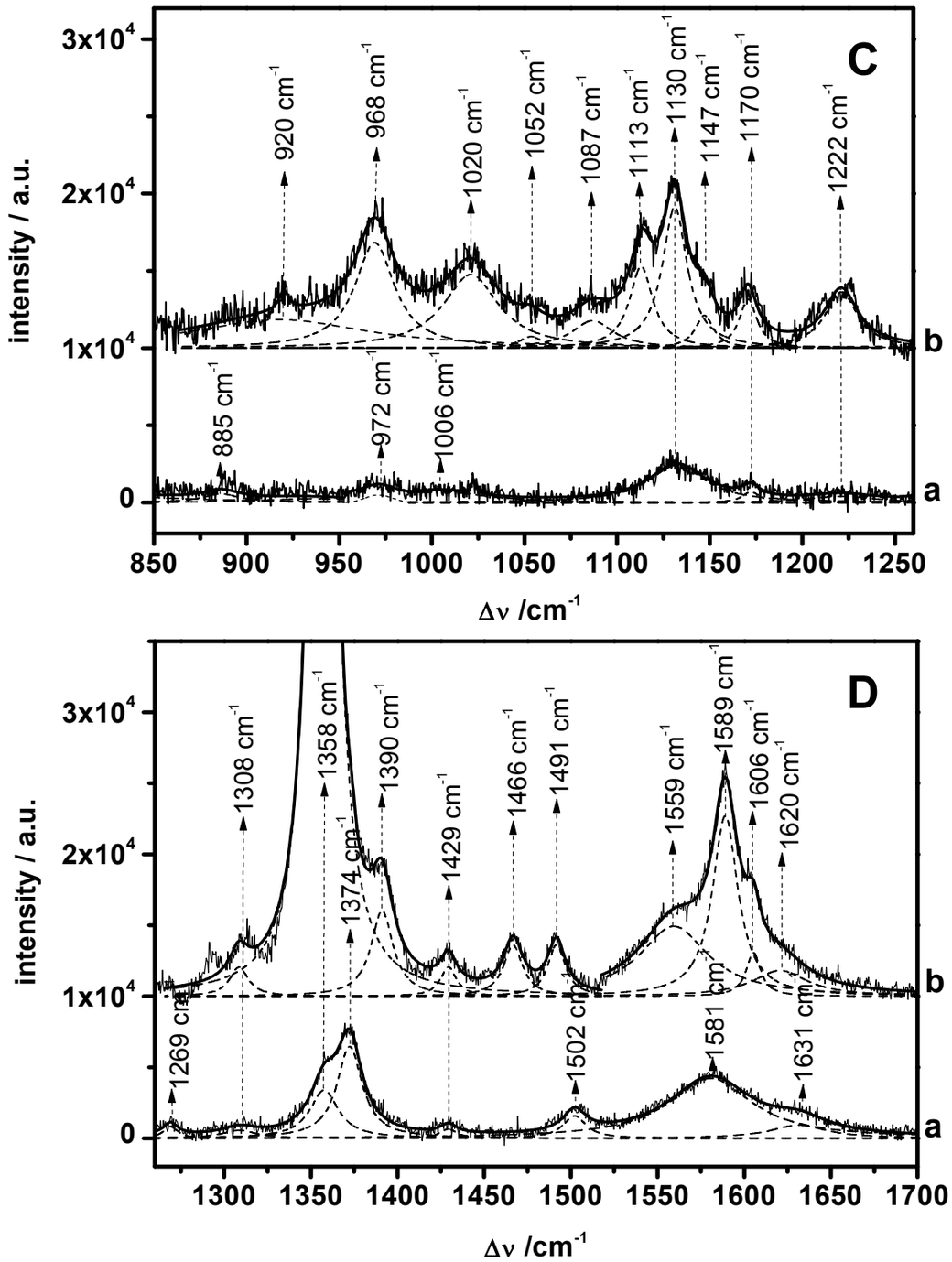

Fig. 4. **SERR spectra of the bc_1 complex** adsorbed onto a functionalized electrode and reconstituted into a bilayer lipid membrane (see Fig.1) with ubiquinone Q_{10} added, recorded under anaerobic conditions at oxidizing potential 250 mV (a) and reducing potential -400 mV (b) in the low- (A), the mid- (B,C) and high frequency region (D). Deconvoluted spectra (dashed lines) and envelope (solid line).

frequency	mode assignment	redox state
343	$\nu'_8(b_H+c_1)$, $\nu_8(b_H+c_1)$	red, ox
356	$\nu'_{50}(c_1)$	red
635	$\nu'_{48}(c_1)$	red
650	$\gamma'_{20}(c_1)$	red
663	$\gamma'_{20}(c_1)$	red
681	$\nu'_7(b)$, $\nu_7(b)$	red, ox
697	$\nu'_7(c_1)$	red
716	$\gamma'_5(b+c_1)$	red, ox
747	$\nu'_{15}(b+c_1)$	red, ox
783	$\nu'_6(c_1)$	red, ox
920	$\nu'_{46}(c_1)$	red
1147	$\nu'_{43}(c_1)$	red
1170	$\nu'_{30}(b_H+c_1)$, $\nu_{30}(b_H+c_1)$	red, ox
1358	$\nu'_4(b+c_1)$	red, ox
1374	$\nu_4(b+c_1)$	ox
1390	$\nu'_{29}(b+c_1)$	red
1466	$\nu'_{28}(b+c_1)$	red
1491	$\nu'_3(b+c_1)$	red
1502	$\nu_3(b+c_1)$	ox
1559	$\nu'_{38}(b+c_1)$	red
1581	$\nu'_2(b+c_1)$, $\nu_2(b+c_1)$	ox
1589	$\nu'_2(c_1)$, $\nu_2(c_1)$	red
1606	$\nu'_{37}(b+c_1)$	red
1620	$\nu'_{10}(c_1)$	red
1631	$\nu_{10}(b+c_1)$	ox

frequency	mode assignment	redox state
263	$\nu'_9(b)$	ox
265	$\nu'_9(b)$	red
377	$\delta'_{CPr}(b)$, $\delta'_{CPr}(b)$	red
403	$\delta'_{CCaCb2,4}(c_1)$	red
407	$\delta'_{CCVn}(b_L)$, $\delta_{CCVn}(b_L)$	ox
416	$\delta'_{CCVn}(b_H)$, $\delta_{CCVn}(b_H)$	red
681 / 696	$\nu'_{CS}(c_1)$, $\nu_{CS}(c_1)$	red, ox
968	$\delta'_{CPr}(b+c_1)$, $\delta_{CPr}(b+c_1)$	red
972	$\delta'_{CPr}(b+c_1)$, $\delta_{CPr}(b+c_1)$	ox
1006	$\delta'_{CVn}(b)$, $\delta_{CVn}(b)$	ox
1087	$\delta'_{CCH3}(c_1)$	red
1113	$\nu'_5(b+c_1)$	red
1130	$\nu'_{14}(b+c_1)$, $\nu_{14}(b+c_1)$	red, ox
1222	$\nu'_{13}(b)$, $\nu_{13}(b)$	red, ox
1308	$\delta'_{CHVn}(b)$	red, ox
1429	$\delta'_{CH2Vn}(b)$	red, ox

Table 2. Frequency (cm^{-1}) of Heme Skeletal Modes (left) and Peripheral Heme Modes (right) observed in SERRS of electrochemically reduced/ oxidized bc_1 complex. ν'_x, δ'_x, γ'_x, ν_x, δ_x, γ_x correspond to the reduced and oxidized state, respectively.

Only two bands at 1308 cm^{-1} and at 1429 cm^{-1} occur in the high frequency region, which originate from peripheral heme modes of the b hemes, δ_{CHVn} and δ_{CH2Vn}, respectively. We found only one band at 1269 cm^{-1} in the high frequency region, which was not considered in previous studies.(Le Moigne, Schoepp et al. 1999)

In summary, the high frequency region contains bands, which originate from all types of hemes. Of particular significance are the marker bands at 1374 cm^{-1} and at 1358 cm^{-1} indicating the redox state of all of the hemes. We conclude therefrom that the bc_1 complex is fully reduced within this particular potential window. However, applying Soret excitation in this particular region it is hard to distinguish between signals from different cytochromes. Nevertheless some modes of this region, such as the ν_2, ν_3, ν_4 and ν_{10} mode give useful information on oxidation and spin state.

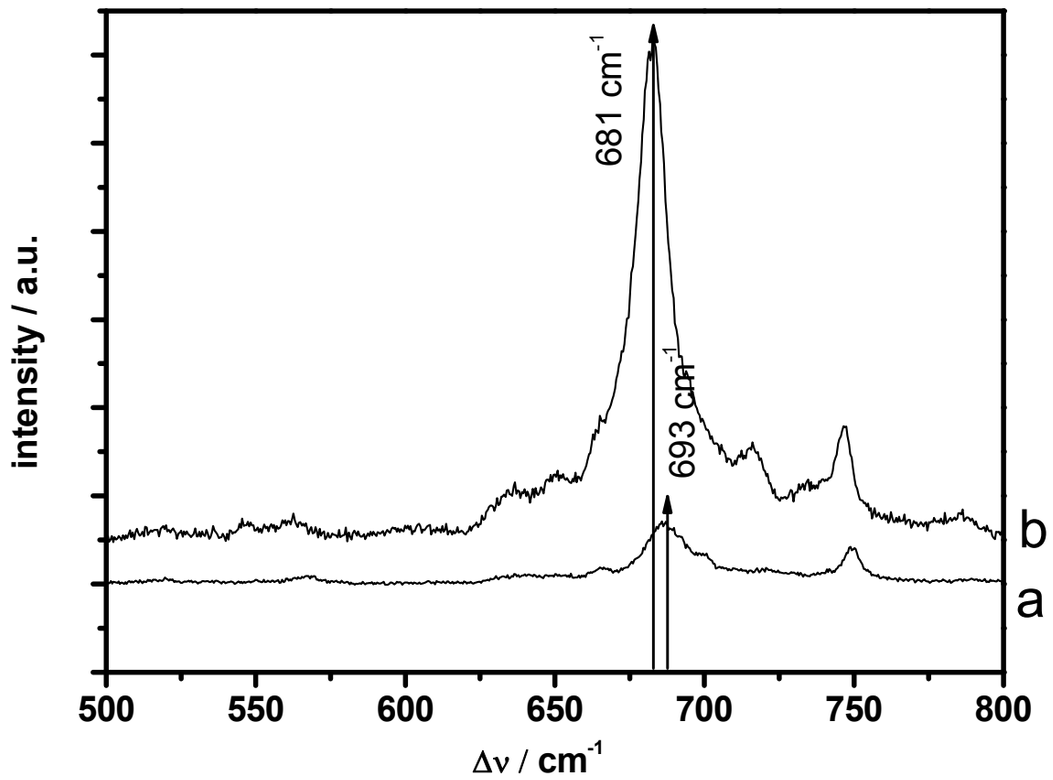

Fig. 5. **Comparison between SERRS in the low frequency region** of reduced cytochrome c (a) and reduced bc_1 complex (b) under anaerobic conditions recorded at -400 mV vs. SHE.

Potentiometric titration

Based on these results, potentiometric titrations were conducted followed by SERRS, i.e. the potential was altered stepwise between +200 mV and -400 mV. Fig. 6 shows the spectra as a function of potential, in the spectral range 1200 - 1770 cm^{-1} (A) and 250 - 970 cm^{-1} (B). The most prominent band refers to the ν_4 mode, a skeletal heme mode of all the hemes, b_L, b_H and c_1, present in the bc_1 complex. The discrete shift from 1374 cm^{-1} to 1357 cm^{-1} indicates that the oxidized form is progressively transformed into the reduced form, respectively. At +200 mV and -300 mV the hemes seem to be completely oxidized and reduced, respectively. Closer inspection of the spectra even at slightly higher and lower potentials, show small contributions of the reduced form at the positive edge of the potential window, whereas the oxidized form seems to be completely removed at -400 mV (compare Fig. 4D spectra a and b showing the deconvoluted SERR spectra in the fully oxidized and reduced state of the enzyme, respectively). We can conclude that the reduction of all the hemes does take place under our experimental conditions.

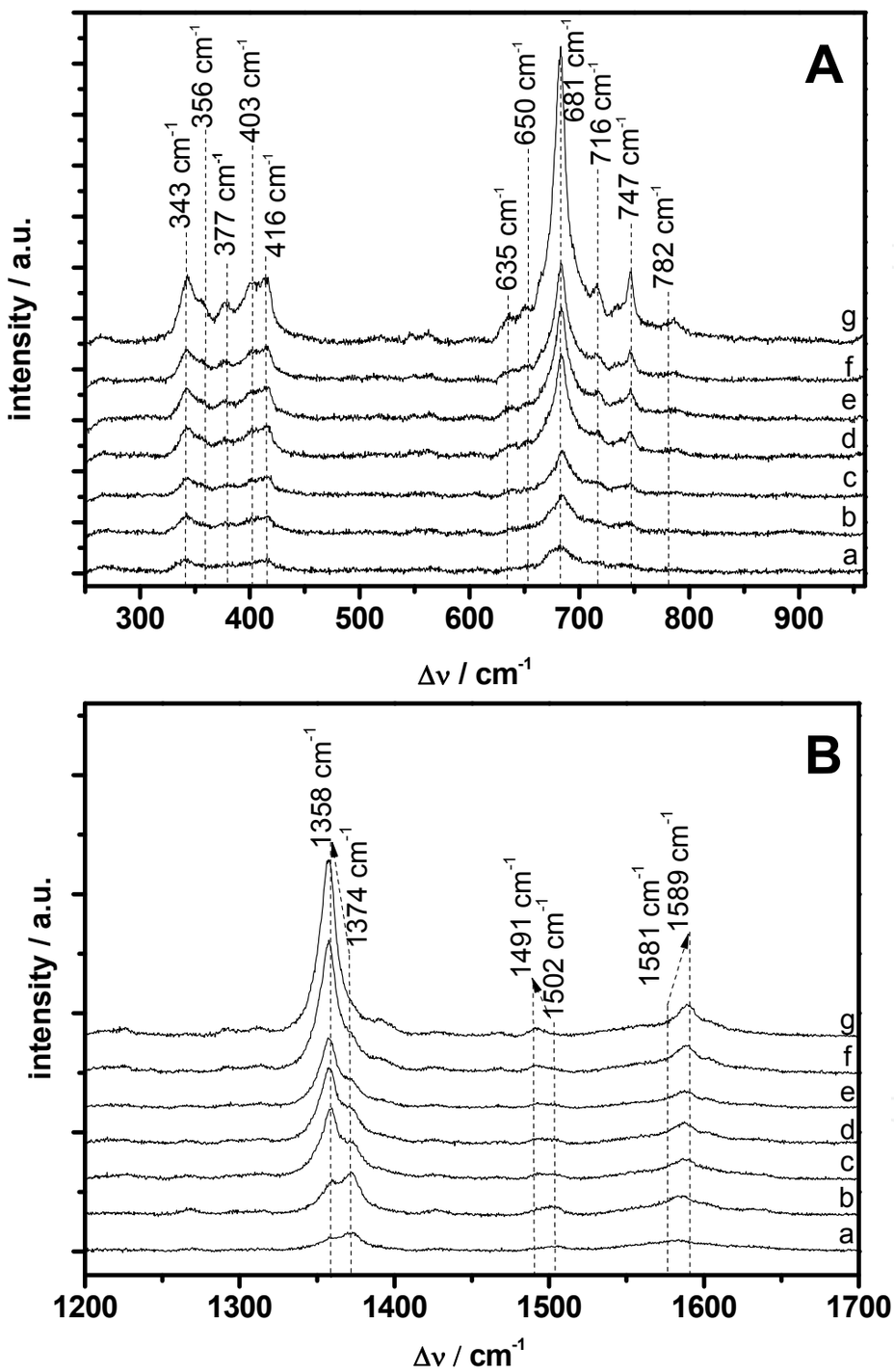

Fig. 6. **SERR spectra of the bc_1 complex** adsorbed onto a functionalized electrode and reconstituted into a bilayer lipid membrane (see Fig.1) with additional ubiquinone Q_{10} recorded under anaerobic conditions as a function of potential taken at 200 mV (a), 100 mV (b), 0 mV(c), -130 mV (d), -150 mV (e), -170 mV (f) and -300 mV (g) for the lower- (A) and the higher frequency region (B).

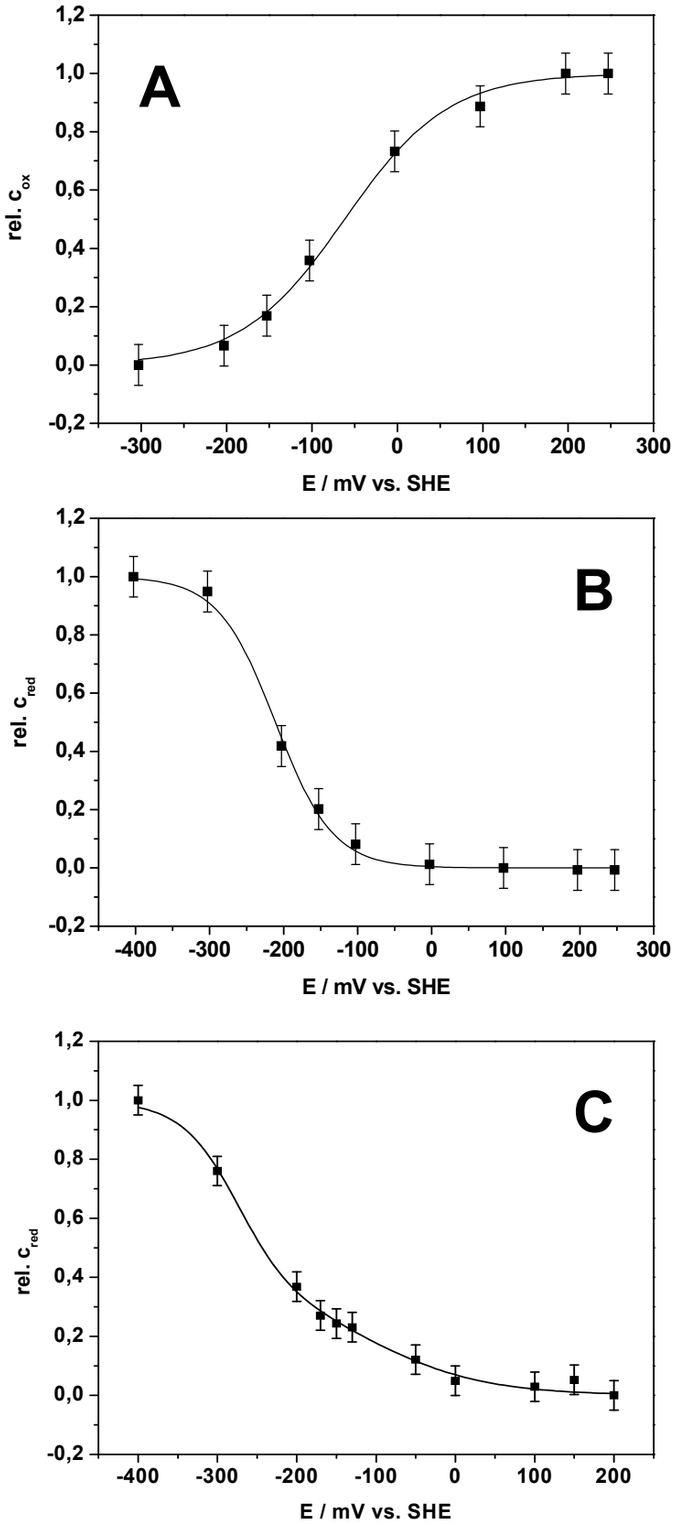

Fig. 7. **Normalized concentration versus potential plots** derived from the ν_4 (A) and ν'_4 mode (B) and the ν'_7 mode (C).

The intensities of the bands referring to ν'_4 and ν_4 correspond to the relative concentration of reduced and oxidized species. Based on this relation we plotted the normalized concentrations of each species as a function of potential (Figure 7). The sigmoid function

$$\text{rel } c_{red} = \frac{1}{\exp\left(\left(E\text{-}E_{ip}\right)\frac{nF}{RT}\right)+1}$$

was fitted to the data, where rel c_{red} is the relative concentration derived from the intensity I_{SERRS} of the bands at 1359 and 1374 cm^{-1}, respectively. E_{ip} is the potential of the inflection point, which reflects the midpoint potential E_m of the redox center, and φ is a scaling factor. Ideally, $\varphi = RT/F \approx 26$ mV, and $E_{ip} = E_m$ in accordance with the Nernst equation. Evaluating the band of ν'_4 revealed a midpoint potential of E_m = -211 mV and a scaling factor of φ = 38 mV (see Fig. 7B). The evaluation of the band according to ν_4 resulted in E_m = -62 mV and a scaling factor of φ = 61 mV (see Fig. 7A). The sigmoid functions obtained as a function of potentials clearly indicate that electrochemical ET into the enzyme does take place. However, we see different E_m values depending on the the band used for the evaluation. This can be explained in terms of different contributions of the three different heme species to the two marker bands.

This assumption is consistent with the potential dependence of a band that is truely selective, such as the band at 681 cm^{-1}, which had been shown above to represent only the b hemes. In this case equation 2

$$\text{rel } c_{red} = \frac{1-c_{1-2}}{\exp\left(\left(E-E_{ip,1}\right)\frac{nF}{RT}\right)+1} + \frac{c_{1-2}}{\exp\left(\left(E-E_{ip,2}\right)\frac{nF}{RT}\right)+1}$$

had to be used to be fitted to the data, showing a two-step process (Fig. 7C) with two inflection points, E_{m1} = -275 mV and E_{m2} = -111 mV. $c_{1\text{-}2}$ denotes the relative concentration of reduced species at the first reduction step. E_{m1} and E_{m2} correspond roughly to the two different E_m values found for the overall marker bands ν_4 described above. Concerning the different heights of the steps, they have to be considered in terms of the sensitivity of the band amplitude from the electric field, rather than in terms of different concentrations. Other bands gave a similar result (not shown), e.g. the bands at 343 and 403 cm^{-1}. One could speculate about a stepwise reduction, for example of the b hemes. The two E_m values, however, are still within the potential window comprising ubisemiquinone rather than ubihydroquinone. This had been shown above (see the CVs Fig. 3) to be reduced at more negative potentials.

4. Conclusion

In general, SERR spectra obtained by electrochemical reduction/oxidation of the bc_1 complex adsorbed to the SERR-active surface correspond to the spectra of the solubilized enzyme.(Le Moigne, Schoepp et al. 1999) Therefore we feel entitled to conclude from our results that electrochemical reduction/oxidation of all of the hemes of the bc_1 complex does take place. However, direct electron transfer to one of the hemes, for example cytochrome c_1, which is nearest to the surface, seems to be excluded. Instead the hemes appear to take up

the electrons via ubiquinone. Q_{10}, on the other hand, seems to exchange electrons with the electrode, even though the lipid phase is separated from the surface by about 3 nm as deduced from the dimensions of the hydrophilic and hydrophobic domain of the bc_1 complex. However, Q_{10} will distribute between lipid and protein matrix where it may find a tunnel pathway to the electrode, possibly via c_1 which is closest to the electrode (Fig. 1). This would explain the electrochemical reduction of Q_{10} taking place in two steps at around –350 mV and -550 mV. The two steps are considered in terms of the ubisemiquinone and ubihydroquinone species, respectively. As deduced from these potentials, ubisemiquinone alone appears to mediate electron transfer into the hemes. Potentials as highly negative as –600 mV required for the reduction to ubihydroquinone are obviously not needed to reduce the hemes. However, within the potential window investigated the hemes are possibly also reduced in two steps at around -90 mV and around -200 mV each. The first value corresponds quite nicely to midpoint potentials reported for the b hemes, whereas the second one was not reported so far. In this context, we have to bear in mind that we are dealing with the electrochemical situation where reduction/oxidation may take place far from the thermodynamic potential due the kinetic limitations. This applies in particular to the reduction ubiquinone (Q) to ubisemiquinone ($Q\bullet^-$) and later to ubihydroquinone (Q^{2-}) the peak potentials of which are highly likely shifted to negative potentials. A large variety of midpoint potentials of the $Q/Q\bullet^-$ and the $Q\bullet^-/Q^{2-}$ couple were reported in biochemical literature varying from -600 mV to -160 mV for $Q/Q\bullet^-$ and +800 mV to +280 mV for $Q\bullet^-/Q^{2-}$(Osyczka, Moser et al. 2005; Grammel and Ghosh 2008). In these cases the $Q\bullet^-/Q^{2-}$couple is considered to be at a higher (more positive) potential than the $Q/Q\bullet^-$ couple. This is highly unlikely not only in the light of the present results, but also with respect to standard potentials known from electrochemical literature. For example the standard potential of $BQ/BQ\bullet^-$ and the $BQ\bullet^-/BQ^{2-}$ couples of benzoquinone are given in a textbook as -540 mV and -140 mV, respectively, however, in a non-aqueous solution (Bard and Faulkner 2001). Irrespective of the absolute values, the $Q/Q\bullet^-$ is always at a higher potential than the $Q\bullet^-/Q^{2-}$ couple, consistent with thermodynamics. The uptake of the first electron requires less energy than that of the second electron. We deduce from this consideration that the peak at around -350 mV corresponds to the $Q/Q\bullet^-$ couple whereas the peak at -550 mV corresponds to the $Q\bullet^-/Q^{2-}$ couple of ubiquinone Q_{10} at pH = 7. Unfortunately, midpoint potentials cannot be deduced from these data since a scan rate study is not feasible due the disappearance of the peaks with time. We can conclude, however, that under our experimental conditions, ubisemiquinone alone is sufficient to reduce the hemes and consequently also cyt c_1, which has a more positive potential anyway. The occurrence of the ubisemiquinone is consistent with the corrected version of the Q cycle brought forward by the group of Dutton.(Osyczka, Moser et al. 2005) In this version the bifurcation of the electron pathway to FeS and cyt c_1 on the one hand and the b hemes on the other occurs simultaneously at the Q_0 site, with ubisemiquinone having a negligible lifetime. Interestingly, we observe the ubisemiquinone only with the bc_1 complex immobilized by electrostatic attraction as described above. In this case we consider the cyt c_1 side directed towards the electrode, bearing in mind that speculations regarding orientation are merely tentative. Anyhow, bifurcation is prevented because cyt c_1 is in the reduced state together with ubiquinone Q_{10}. Hence the $Q\bullet^-$ species can be observed in the CV. This could be considered as an indication of the Q_0 site, particularly since ubisemiquinone is quickly consumed by the enzyme, see the evolution of the CVs with time (Fig.3, inset). In the case of

the bc_1 complex immobilized via a his-tag attached to the side opposite to c_1 we observe only the two-electron uptake directly to ubihydroquinone at around -550 mV (data not shown) without the intermediate step to the ubisemiquinone. This is consistent with data from the Jeuken group, who investigated ubiquinone Q_{10} incorporated in a tethered bilayer lipid membrane. They also observe the two-electron uptake at potentials of -400 mV to -500 mV depending on protonation states.(Jeuken, Bushby et al. 2006)

Summarizing hemes b_L, b_H and c_1 are reduced via QH• under electrochemical control. However, catalytic currents were not observed, which is not surprising considering that cyt c is also reduced at the same potential together with the b hemes.

As regards the SERR spectra, that we observe under these conditions, they show a much improved resolution and sensitivity as compared to the spectra in solution. This can be explained in terms of the surface enhancement effect described earlier for a silver electrode modified with Ag nanoparticles.(Grosserueschkamp, Nowak et al. 2009) Different mechanisms contribute to the enhanced Raman scattering of molecules adsorbed on rough metal substrates. The electro-magnetic enhancement effect (Jeanmaire and Van Duyne 1977) (EMEE) and the chemical enhancement effect (CEE)(Albrecht and Creighton 1977), the latter also known as charge transfer effect, are of great interest in this context. The EMEE is based on collective electron oscillations in resonance with the exciting laser wavelength yielding high electromagnetic field enhancement in the proximity of the metal surface.(Moskovits 1985) In the literature such electron oscillations are often referred to as localized surface plasmons (LSP), particularly if they are excited within nanoscopic metal structures such as colloids or rough surface bumps. The EMEE is capable of enhancing the intensity of Raman spectra of all molecules in close proximity to the metal substrate. Contrary to the EMEE the CEE only occurs if the probed molecules are adsorbed on the surface. The underlying mechanism is a charge-transfer resonance between the metal substrate and the adsorbed molecule. Assuming the Fermi level of the metal is located between the ground state and an excited state of the molecule, charge transfer transitions from the Fermi level to the excited state, as well as transitions from the ground state to the Fermi level, can contribute to the CEE.(Lombardi, Birke et al. 1986; Lombardi and Birke 2008)

Even though these effects are well understood, it is difficult to differentiate between contributions from EMEE and CEE. EM enhancement has to be considered particularly if the molecules are adsorbed to a metal substrate modified with nanoparticles. The Ag surface used in the present study had been optimized with respect to the enhancement factor using cytochrome c as a benchmark system.(Grosserueschkamp, Nowak et al. 2009) The good enhancement could be confirmed in the case of the bc_1 complex. In this case, the enhancement is further reinforced by externally applied electric fields. This is clearly demonstrated by the comparatively high amplitude of the bands, particularly in the negative range of potentials. This is due to electrochemical properties of the Ag surface, which is sensitive to anodic dissolution at the positive edge of the potential window. Therefore, the potential window extends much more into the range below zero than above zero. In addition chemical enhancement may also play a role, particularly since the molecules are arranged on the surface in a strict orientation due to electrostatic interaction. This orientation is further supported by the lipid molecules inserted in between the protein entities. These effects taken together seem to overcome the traditionally poor signal-to-noise ratios in Raman spectra which are an inherent problem of the weak scattering process, particularly since in spectro-electrochemistry we are probing merely a monolayer of molecules.

As a further advantage of spectro-electrochemistry, the redox state of the protein can be easily manipulated, so that a titration can be conducted. The regular changes recorded in this case further highlight the quality of the spectra which can be presented without any additional treatment.

Since the marker band for the ν_4 mode shows sensitivity to the redox state, we conclude, that the potential dependent changes in intensity of the displayed bands are not exclusively generated by the charge transfer mechanism but also by a genuine reduction and oxidation of the hemes.

6. Acknowledgement

We are grateful to Carola Hunte, University of Freiburg, Germany, for critical discussions of the results and also for providing us with the sample of the bc_1 complex the yeast *Saccharomyces cerevisiae*.

7. References

Albrecht, M. and J. A. Creighton (1977). "Anomalously Intense Raman-Spectra of Pyridine at a Silver Electrode." JACS 99(15): 5215-5217.

Bard, A. J. and L. R. Faulkner (2001). Electrochemical Methods: Fundamentals and Applications, John Wiley & Sons.

Berry, E. A., L. S. Huang, et al. (2004). "X-Ray Structure of Rhodobacter Capsulatus Cytochrome bc (1): Comparison with its Mitochondrial and Chloroplast Counterparts." Photosynth Res 81(3): 251-75.

Chase, B. and B. Parkinson (1991). "A study of the wavelength and potential dependence of surface enhanced Raman scattering on copper, silver, and gold electrodes." The Journal of Physical Chemistry 95(20): 7810-7813.

Choi, S. and T. G. Spiro (1983). "Out-of-plane deformation modes in the resonance Raman spectra of metalloporphyrins and heme proteins." JACS 105(11): 3683-3692.

Feng, M. and H. Tachikawa (2008). "Surface-Enhanced Resonance Raman Spectroscopic Characterization of the Protein Native Structure." Journal of the American Chemical Society 130(23): 7443-7448.

Friedrich, M. G., J. W. Robertson, et al. (2008). "Electronic wiring of a multi-redox site membrane protein in a biomimetic surface architecture." Biophys J 94(9): 3698-3705.

Gao, F., H. Qin, et al. (1998). "Q-band resonance Raman spectra of oxidized and reduced mitochondrial bc1 complexes." Biochemistry 37(27): 9751-8.

Grammel, H. and R. Ghosh (2008). "Redox-State Dynamics of Ubiquinone-10 Imply Cooperative Regulation of Photosynthetic Membrane Expression in *Rhodospirillum rubrum*." Journal of Bacteriology 190, No.14: 4912-4921.

Grosserueschkamp, M., M. G. Friedrich, et al. (2009). "Electron transfer kinetics of cytochrome c probed by time-resolved surface-enhanced resonance Raman spectroscopy." J Phys Chem B 113(8): 2492-7.

Grosserueschkamp, M., C. Nowak, et al. (2009). "Silver Surfaces with Optimized Surface Enhancement by Self-Assembly of Silver Nanoparticles for Spectroelectrochemical Applications." Journal of Physical Chemistry C 113(41): 17698-17704.

Hobbs, D. D., A. Kriauciunas, et al. (1990). "Resonance Raman spectroscopy of cytochrome bc1 complexes from Rhodospirillum rubrum: initial characterization and reductive titrations." Biochim Biophys Acta 1018(1): 47-54.

Hu, S. (1993). "Comment on Cooper and Kennedy Flow-Insensitive Interprocedural Summary Information Computation Algorithm." Sigplan Notices 28(5): 3-8.

Hu, S., I. K. Morris, et al. (1993). "Complete assignment of cytochrome c resonance Raman spectra via enzymic reconstitution with isotopically labeled hemes." Journal of the American Chemical Society 115(26): 12446-12458.

Hu, S., K. M. Smith, et al. (1996). "Assignment of Protoheme Resonance Raman Spectrum by Heme Labeling in Myoglobin." Journal of the American Chemical Society 118(50): 12638-12646.

Hunte, C., J. Koepke, et al. (2000). "Structure at 2.3 A resolution of the cytochrome bc(1) complex from the yeast Saccharomyces cerevisiae co-crystallized with an antibody Fv fragment." Structure 8(6): 669-84.

Jeanmaire, D. L. and R. P. Van Duyne (1977). "Surface raman spectroelectrochemistry: Part I. Heterocyclic, aromatic, and aliphatic amines adsorbed on the anodized silver electrode." Journal of Electroanalytical Chemistry 84(1): 1-20.

Jeuken, L. J. C., R. J. Bushby, et al. (2006). "Proton transport into a tethered bilayer lipid membrane." Electrochemistry Communications 9(4): 610-614.

Kitagawa, T., Y. Kyogoku, et al. (1975). "Resonance Raman scattering from hemoproteins. Effects of ligands upon the Raman spectra of various C-type cytochromes." J Biochem 78(4): 719-28.

Kitagawa, T., Y. Ozaki, et al. (1978). "Resonance Raman studies on the ligand-iron interactions in hemoproteins and metallo-porphyrins." Adv Biophys 11: 153-96.

Kozlowski, P. M., J. R. Bingham, et al. (2008). "Theoretical Analysis of Core Size Effect in Metalloporphyrins." Journal of physical Chemistry A 112(50): 12781-12788.

Lange, C. and C. Hunte (2002). "Crystal structure of the yeast cytochrome bc1 complex with its bound substrate cytochrome c." Proc Natl Acad Sci U S A 99(5): 2800-5.

Lange, C., J. H. Nett, et al. (2001). "Specific roles of protein-phospholipid interactions in the yeast cytochrome bc1 complex structure." EMBO J 20(23): 6591-600.

Le Moigne, C., B. Schoepp, et al. (1999). "Distinct structures and environments for the three hemes of the cytochrome bc1 complex from Rhodospirillum rubrum. A resonance Raman study using B-band excitations." Biochemistry 38(3): 1066-76.

Lombardi, J. R. and R. L. Birke (2008). "A unified approach to surface-enhanced Raman spectroscopy." Journal of Physical Chemistry C 112(14): 5605-5617.

Lombardi, J. R., R. L. Birke, et al. (1986). "Charge-transfer theory of surface enhanced Raman spectroscopy: Herzberg--Teller contributions." The Journal of Chemical Physics 84(8): 4174-4180.

Moskovits, M. (1985). "Surface-Enhanced Spectroscopy." Review of Modern Physics 57(3): 783-826.

Nowak, C., D. Schach, et al. (2009). "Oriented Immobilization and Electron Transfer to the Cytochrome c Oxidase." J.Solid State Electrochemistry DOI 10.1007/s10008-010-1032-x.

Osawa, M., N. Matsuda, et al. (1994). "Charge transfer resonance Raman process in surface-enhanced Raman scattering from p-aminothiophenol adsorbed on silver: Herzberg-Teller contribution." The Journal of Physical Chemistry 98(48): 12702-12707.

Osyczka, A., C. C. Moser, et al. (2005). "Fixing the Q cycle." TRENDS in Biochemical Sciences 30 No.4: 176-182.

Pálsdóttir, H. and C. Hunte (2003). Purification of the Cytochrome bc1 Complex from Yeast. Membrane Protein Purification and Crystallization (Second Edition). H. Carola, J. Gebhard Von and S. Hermann. San Diego, Academic Press: 191-203.

Palsdottir, H., C. G. Lojero, et al. (2003). "Structure of the yeast cytochrome bc1 complex with a hydroxyquinone anion Qo site inhibitor bound." J Biol Chem 278(33): 31303-11.

Schach, D., C. Nowak, et al. (2010). "Modeling direct electron transfer to a multi-redox center protein: cytochrome c oxidase." J. of Electroanalytical Chemistry DOI10.1016/j.jelechem.2010.07.009.

Solmaz, S. R. and C. Hunte (2008). "Structure of complex III with bound cytochrome c in reduced state and definition of a minimal core interface for electron transfer." J Biol Chem 283(25): 17542-9.

Spiro, T. G. (1975). "Resonance Raman spectroscopic studies of heme proteins." Biochim Biophys Acta 416(2): 169-89.

Spiro, T. G. (1978). "Resonance Raman spectra of hemoproteins." Methods Enzymol 54: 233-49.

Spiro, T. G. (1988). Biological applications of Raman spectroscopy, Vol. 3: Resonance Raman spectra of heme proteins and other metalloproteins.

Spiro, T. G., R. S. Czernuszewicz, et al. (1989). "Metalloporphyrin structure and dynamics from resonance raman spectroscopy." Coordination Chemistry Reviews 100: 541-571.

Spiro, T. G. and T. C. Strekas (1974). "Resonance Raman spectra of heme proteins. Effects of oxidation and spin state." J Am Chem Soc 96(2): 338-45.

Xia, D., C. A. Yu, et al. (1997). "Crystal structure of the cytochrome bc1 complex from bovine heart mitochondria." Science 277(5322): 60-6.

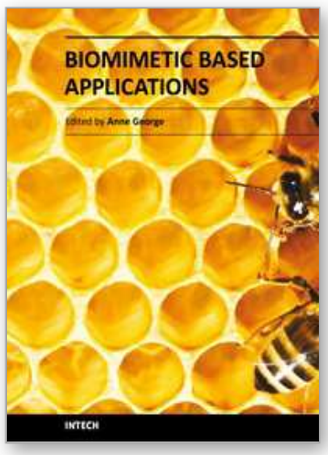

Biomimetic Based Applications

Edited by Prof. Marko Cavrak

ISBN 978-953-307-195-4
Hard cover, 572 pages
Publisher InTech
Published online 26, April, 2011
Published in print edition April, 2011

The interaction between cells, tissues and biomaterial surfaces are the highlights of the book "Biomimetic Based Applications". In this regard the effect of nanostructures and nanotopographies and their effect on the development of a new generation of biomaterials including advanced multifunctional scaffolds for tissue engineering are discussed. The 2 volumes contain articles that cover a wide spectrum of subject matter such as different aspects of the development of scaffolds and coatings with enhanced performance and bioactivity, including investigations of material surface-cell interactions.

How to reference

In order to correctly reference this scholarly work, feel free to copy and paste the following:

Denise Schach, Marc Großerüschkamp, Christoph Nowak, Wolfgang Knoll and Renate L. C. Naumann (2011). Spectro-Electrochemical Investigation of the bc1 Complex from the Yeast Saccharomyces cerevisiae using Surface Enhanced B-Band Resonance Raman Spectroscopy, Biomimetic Based Applications, Prof. Marko Cavrak (Ed.), ISBN: 978-953-307-195-4, InTech, Available from: http://www.intechopen.com/books/biomimetic-based-applications/spectro-electrochemical-investigation-of-the-bc1-complex-from-the-yeast-saccharomyces-cerevisiae-usi

INTECH
open science | open minds

InTech Europe
University Campus STeP Ri
Slavka Krautzeka 83/A
51000 Rijeka, Croatia
Phone: +385 (51) 770 447
Fax: +385 (51) 686 166
www.intechopen.com

InTech China
Unit 405, Office Block, Hotel Equatorial Shanghai
No.65, Yan An Road (West), Shanghai, 200040, China
中国上海市延安西路65号上海国际贵都大饭店办公楼405单元
Phone: +86-21-62489820
Fax: +86-21-62489821

IntechOpen